An investigation on effects of flight altitude, forward and inside overlaps on calibration parameters in UAV images

Midya Rostami [1], Marjan Ahangarha [2], Masood Varshosaz [3*]

1 PhD. candidate of Remote Sensing, Department of Photogrammetry and Remote Sensing, Faculty of Geodesy and Geomatics Engineering, K.N Toosi University of Technology, Tehran, Iran, midyalab@gmail.com

2 PhD. candidate of Remote Sensing, Department of Photogrammetry and Remote Sensing, Faculty of Geodesy and Geomatics Engineering, K.N. Toosi University of Technology, Tehran, Iran, m.ahangarha@email.kntu.ac.ir

3* Institute of Artificial Intelligence, Shaoxing University, Shaoxing, China and Dept. of Photogrammetry, K.N. Toosi University of Technology, Tehran, Iran, varshosazm@usx.edu.cn (*corresponding author)

Keywords: UAV, Metashape, Reprojection Error, Cloud Point

Abstract

Accurate 3D models obtained through the combined use of photogrammetry and unmanned aerial vehicles (UAVs) have become highly valuable in various industries. These models offer a wealth of information and serve as effective tools for diverse applications. UAV photogrammetry technology provides a cost-efficient and productive solution for generating precise 3D models. Flight altitude and forward and side overlaps are critical factors influencing the production of these models, as they directly impact calibration parameters and overall accuracy. In this study, we conducted experiments using a DJI Phantom 4 Pro UAV at flight altitudes of 60 m, 90 m, and 120 m, with forward and side overlaps set at 60%, 70%, and 80%. By analyzing the residual errors of 3D sparse points generated from tie points, a significant finding emerged. The combination of a 90 m flight altitude and a 60% forward and side overlap yielded the most favorable results in terms of residuals, with a value of 0.1954 pixels and an estimated focal length of 8.7999 mm. These findings highlight the optimized accuracy and precision achieved by this particular combination in generating 3D models.

1. Introduction

Nowadays 3D models are the most important tools in industries for the creation and Visual perception of the real world. Photogrammetry is a technique used to cre-ate 3D models by capturing and analysing a series of photographs of an object or environment. It plays a crucial role in various industries, offering accurate data collection, cost and time efficiency, versatility, realistic visualizations, and future potential (Karami et al. 2022). Photogrammetry allows for the collection of highly accurate data from imagery, making it essential in fields such as architecture. It is a cost-effective and time-efficient alternative to traditional 3D modeling methods. Photogrammetry can be applied to various use cases and industries, enabling the creation of highly realistic 3D models. Unmanned Aerial Vehicles (UAVs) significantly impacted the field of photogrammetry in recent years due to the very low cost of flight, flight at low altitude (Ma et al. 2022), ease of use and use of sensors LiDAR (Light Detection and Ranging) (Curcio et al. 2022) and depth sensor (Rueda-Ayala et al. 2022), magnetometer sensor (Zahran et al. 2019), hyperspectral sensor (Imangholiloo et al. 2019), etc.) and different cameras (metric and non-metric cameras (Rokhmana et al. 2019).

One of the main advantages of using UAVs for photo-grammetry is the ability to capture high-resolution imagery. UAVs are equipped with cameras that can capture images with a resolution of up to 10 cm per pixel, which is much higher than the resolution of traditional aerial photography. This high resolution allows for more accurate measurement of objects and features in the image, which is crucial for many applications such as engineering and architectural and archaeological (Mo-yano et al. 2020) surveys and 3D modeling (Shahbazi et al 2015; Ruzgienė et al. 2015) topographic mapping and monitoring (Azmi et al. 2014; Goncalves et al. 2015). Another advantage of using UAVs for photogrammetry is the ability to fly at low altitudes (Galkin et al. 2017). This allows for the capture of images with a wide field of view, which is vital for capturing objects or accurate 3d models (Wierzbicki. et al. 2019) However, using UAV also has its own set of challenges. The main chal-lenge is to ensure the accuracy of the images. This can be achieved by using high-quality cameras and lenses, as well as by ensuring that the UAV is stable during flight. Additionally, atmospheric conditions, such as haze or low light conditions, can affect image quality and accuracy. In addition, creating the accurate 3d models needs the calibrated equipment, in most UAVs the camera is non calibrated type.

Camera calibration plays a crucial role in establishing an accurate relationship between object points and their image projections. However, calibration can be challenging due to limitations in flight trajectory options and mechanical stability issues. In photogrammetry, the correct estimation of interior and exterior orientations for each camera station is vital, as it ultimately leads to the creation of a more precise 3D model. In computer vision applications, accurate camera calibration is cru-cial for tasks like 3D reconstruction of model, where precise knowledge of camera parameters and reprojection is essential (Hong et al. 2021). Study on residuals of reprojection error stands as a critical metric for assessing the effectiveness of camera calibration algorithms. It quantifies the disparity between the image points captured and the corresponding points of repro-jected onto the calibrated camera. High reprojection errors indicate poor calibration accuracy, suggesting that the camera parameters are not accurately estimated. This can result in inaccurate measurements and unreliable 3D reconstructions (Hanning et al. 2005; Dai et al. 2014).Reprojection errors can be caused by various factors, such as lens distortion, inaccurate camera intrinsic parameters, and improper calibration pattern detection (Hong et al. 2021; Albarelli et al. 2010). Minimizing

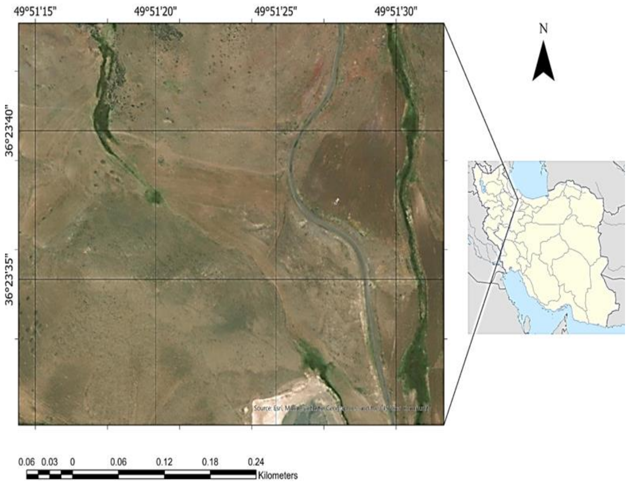

Figure 1. The map of study area

reprojection errors is essential for achieving precise camera calibration (Cvišić, et al. 2022). Residuals of Reprojection errors can be minimized that refine the camera parameters until the observed image points closely match their reprojected positions. This iterative process can helps improve the accuracy of the calibration. In many software applications that utilize structure from motion and block adjustment techniques (such as Agisoft Metashape) to generate 3D models from UAV images, two significant factors come into play:

1.the number of images (forward and side overlaps)

2.the flight altitude.

These factors greatly impact the quality and accuracy of the resulting 3D model. The residual of reprojection errors after block adjustment processes can help to measure these factors. There is paper conducts a comparative experiment on a 3d model of bridge using three overlap configurations [20]. The results suggest that a configuration of 66.7% forward overlap and 50% side overlap is optimal, as it minimizes the number of images while saving mission time for image acquisition and processing. This overlap recommendation may be applicable to 3D reconstruction of other bridge types and buildings with similar components. In one study that investigates the influence of UAV flight direction and camera orientation on positioning accuracy in an urban area. Different flight cases were tested, and it was found that combining multiple sets of images with different flight directions and camera orientations improved overall positional accuracy to a few centimetres. Horizontal accuracy was generally better than vertical accuracy (Wang et al. 2022). One paper presents a pipeline for assessing accuracy using the Roman Amphitheatre of Avella as a case study (Barba et al. 2019). The chosen flight configuration and georeferencing are verified using residuals on ground control points. An outlier detection method considers the statistical distribution of reprojection errors, and a noise reduction filter is implemented using the angle formed by homologous rays to balance usable points and reduce noise in the 3D model. There is study that assesses the impact of flight altitude and overlap degree on the geometric accuracy of 3D point clouds and models generated from UAV images captured over non-textured sandy areas. The results demonstrate that increasing altitude reduces flight time, processing time, and cost while maintaining acceptable geometric accuracy (Elhadary et al. 2022; Elhadary et al. 2022).
Building upon previous research, this study focuses on investigating the effects of flight height, forward over-lap, and side overlap on calibration parameters. By analysing these factors, we aim to gain a deeper under-standing of their impact and how they influence the calibration process.

2. Study Area and Data Acquisition

In this section study area and data acquisition are de-fined and explained.

2.1 Study Area

The study area is located in the mountain range north-west of Qazvin City, the capital of Qazvin province in Iran. The center of study area Situated at latitude of 36°23'37.22"N and longitude of 49°51'22.56"E. The mountain range is characterized by its rugged topogra-phy, comprising steep slopes, and shallow valleys. These landforms offer both challenges and opportuni-ties for photogrammetric analysis, requiring careful consideration of image acquisition and processing tech-niques. While the study area encompasses a vast ex-panse of land, the specific research focus spans an area of 8.39 hectares. Accessibility to the area is facilitated by a network of roads and trails, although the rugged terrain may pose challenges in reaching certain loca-tions. Figure (1) illustrate the map of study area.

2.2 Equipment

The UAV utilized in this research is the DJI Phantom 4 Pro (figure 2), a platform praised for its mechanical shutter, high-resolution camera, long-range abilities, and its compatibility with the 3rd party path planning software for flight planning and image capture. Table (1) illustrates the camera specification of the DJI Phantom 4 Pro. The model of used camera FC6310 is and, in this research the focal length sets on 8.8 mm.

Specification	Details
Sensor	1" CMOS
Effective Pixels (million pixels)	20
Pixel Size (mm)	0.00241228
Field of View	84°
Focal length	8.8 mm / 24 mm (35 mm format equivalent), focus at 1 m - ∞
Aperture	f/2.8 - f/11
ISO Range	Photo: 100 - 3200 (Auto), 100- 12800 (Manual)
Mechanical Shutter Speed (sec)	8 - 1/2000
Electronic Shutter Speed (sec)	8 - 1/8000

Table 1. FC6310 cameras Specification of DJI Phantom 4 Pro

Figure 2. DJI Phantom 4 Pro (Source: http://www.dji.com)

3. Method

As shown in Figure (3), the proposed method has been implemented in five phases. Firstly, UAV data was collected in nadir form with an 80% coverage of both forward and side overlap. Three different flight altitude of 60 m, 90 m, and,120 m was considered for the data collection process.
Subsequently, the images were aligned using Agisoft Metashape software. During this alignment step, the software utilizes the bundle block adjustment. The set-tings in the software for the tie points limitation sets a maximum value of 20,000 while the

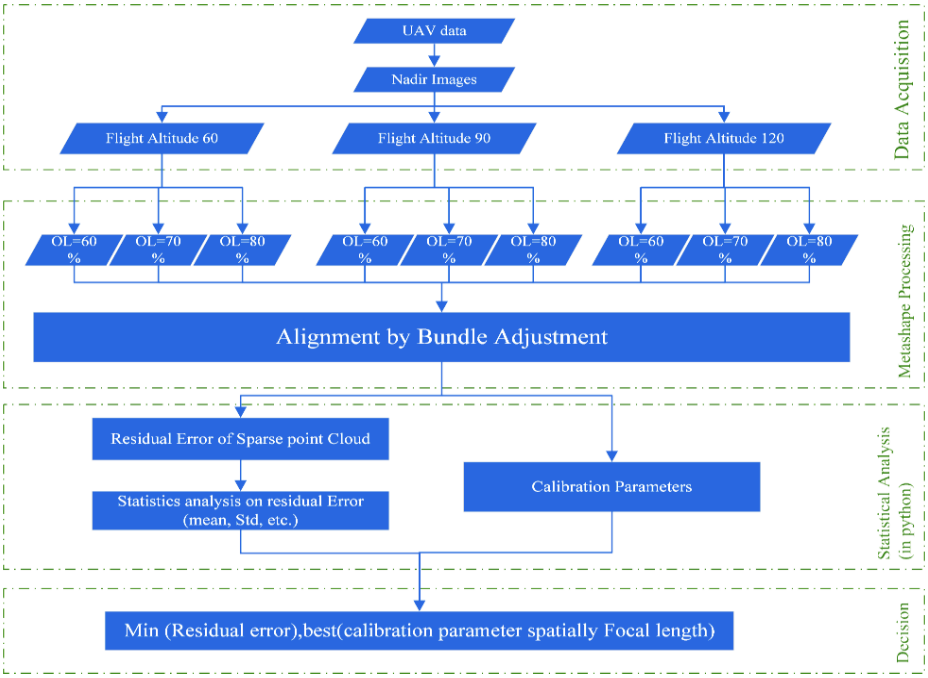

Figure 3. flowchart of the research

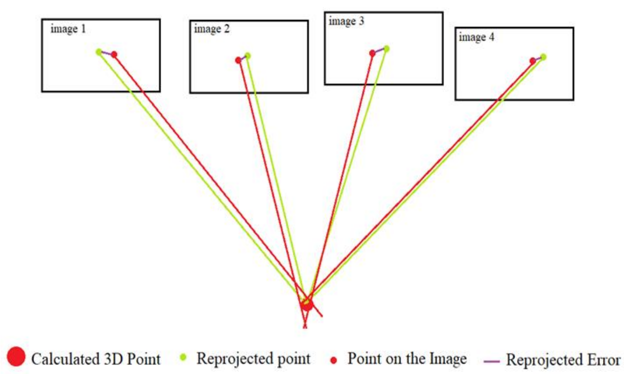

Figure 4. illustration of reprojection and residual error

key points limitation sets a maximum value of 40,000.
Following the alignment, the sparse point cloud is generated based on the tie points obtained from the camera calibration parameters' plane condition.
Next, the residual error values are obtained from the re-projection bundle adjustment, and the check and control errors are calculated using the GCP values for each received model. By utilizing the GCP values for each obtained model, the check and control errors are deter-mined, allowing for the extraction of an appropriate calibration set. All the aforementioned steps were car-ried out for both 60% and 70% forward and side overlap coverage. These two coverage values were extracted from the main coverage. In next section of this article the theory of this research will be explained.

3.1 Concept of Reprojection and Residual Error

Theoretically, when a group of images is aligned using bundle adjustment, the 3D position of a point is com-puted using both the extrinsic and intrinsic parameters of the camera. This computation allows the positions of tie points in the sparse point cloud to be determined. Figure (4) illustrates this process. Based on the quality of the camera and its lens, the 3D coordinates of the points are reprojected onto the corresponding images. For each image, there is a reprojected point and a point on the image itself. The vector between these two points represents the residual error.
Additionally, image residuals serve as a measure of the disparity between the observed positions of control points in an image and their predicted positions based on a model. They provide valuable insights into the accuracy and quality of the photogrammetric model and the analyzed images.
In the end the quality of sparse point depends on the residuals. image residuals serve as indicators of the accuracy and quality of the photogrammetric model and analyzed images

3.2 The Software and Programming

Agisoft Metashape (formerly known as PhotoScan) is professional software used for photogrammetry and 3D modeling. Developed by Agisoft, it processes images to create accurate 3D models and maps (Agisoft et al. 2019). the software utilizes bundle block adjustment to align UAV images. For creating dense points cloud, the tie point matching quality is set to high, ensuring the use of original images without Down sampling. As a result, the exterior and interior calibration parameters of each camera are estimated accurately. Due to table (2) Regarding the Reference Preselection parameter, overlap-ping pairs of photos are selected in Source mode, con-sidering the measured camera locations. The option "Reset current alignment" is chosen, which involves discarding all existing tie, key, and matching points. Consequently, the alignment procedure starts anew from the initial stages. Due to the presence of grass and uni-form texture in the scene, the limitation number of key and tie points are set to 40,000 and 20,000.

After generating the points cloud, a script is written in Python programming language, which is executed in the main program. The purpose of this script is to extract the residual error for each point in dense points cloud, which makes it a map of points and its error rate. In addition, based on formulas of table (3) this program calculates the average error, standard deviation and skewness of the residual errors. In the link in footnote, you can access this script.

Parameter	Setting
Accuracy	High
Generic Preselection	Yes
Reference Preselection	Yes- Source
Reset Current Alignment	Yes
Key Point Limit	40,000
Tie Point Limit	20,000

Table 2. Parameter setting for creating 3D sparce point cloud in Metashape program

Flight Altitude (m)	**60**			**90**			**120**		
Overlaps (%)	**60**	**70**	**80**	**60**	**70**	**80**	**60**	**70**	**80**
Number of images	34	68	136	15	31	63	10	20	40
GSD (cm/px)	1.64	1.64	1.64	2.46	2.46	2.46	3.2	3.2	3.2
Average Residual error (px)	0.1956	0.2209	0.2213	**0.1954**	0.2132	0.2233	0.2292	0.2234	0.2257
Standard Deviation	0.2288	0.2829	0.3115	0.2331	0.2775	0.3063	0.2402	0.2668	0.2927
Skewness	5.9664	6.8147	4.3663	4.7048	5.3305	7.1476	13.5667	9.0930	7.8397
Estimated Focal Length (mm)	8.8170	8.8063	8.8038	**8.7999**	8.7945	8.7958	8.8560	8.7983	8.8151
GCP control error (m)	0.005	0.009	0.014	**0.0017**	0.00164	0.0021	0.00366	0.0041	0.0061
GCP Check error (m)	0.0065	0.0078	0.008	**0.00185**	0.00433	0.0076	0.00243	0.0068	0.0098

Table 3. Parameters that examined at flight altitudes of 60 m, 90 m, 120m and 60%, 70%, 80% forward and side overlaps.

*The bolded values are the best values condition.

Index	**Formula**
1- average error	$\bar{X} = \frac{\sum_i^N Residuals}{N}$
2-standard deviation	$\sigma = \sqrt{\frac{\sum(X_i - \mu)^2}{N}}$
3-skewness	$\tilde{\mu}_3 = \frac{\sum_i^N (X_i - \bar{X})}{(N-1) \times \sigma^3}$

Table 4. statistical indices that used in python script

Were in the table (4) in formula 1 $\bar{X}$ is average error of residuals, in formula 2 σ is standard deviation, μ is the population mean, *N* is the size of the population and, in formula 3 $\tilde{\mu}_3$ is skewness.

4. Results and Discussion

After implementation the data in Metashape software the 3d sparse points were created for three altitudes and three overlaps, the script did run on each 3D models then the results are collected in this part.

Figure (5) illustrates the residual error map for each 3d sparse points cloud for flight altitudes of 60 m, 90 m, 120m and 60%, 70%, 80% forward and side overlaps. It is explicit we can see sparsity in the models that made by overlaps of 60% that is because of the lack of images that have not enough tie points to create model with less sparsity. Although for higher overlaps and altitudes it can see that models are more rigid and tie point residual errors are spread evenly. This is because the number of images has increased and more features for matching have been identified by the software. The amount of skewness, which measures the asymmetry of the error distribution, varies significantly across different flight conditions. This suggests that the distribution of errors can be quite different depending on the specific conditions of the flight. Figure (6) displays the distribution of residual errors for flight altitudes of 60 m, 90 m, and 120 m, with forward and side overlaps of 60%, 70%, and 80%. The range of values differs for each flight altitude and overlap, but most of them fall within the range of 0 to 17.5 pixels.

Interestingly, the 3D sparse points cloud created with a flight altitude of 90 m and a 60% overlap exhibits the smallest range of residuals among all the conditions.

Table (4) and Figure (7) present comparisons of various parameters that were examined at different flight altitudes and overlaps. These parameters include:

1. **Number of Images:** This refers to the total number of images captured during the flight.
2. **Ground Sampling Distance (GSD):** GSD represents the distance between two consecutive pixel centers on the ground. It is a measure of the spatial resolution of the captured images.
3. **Average Residual Error:** This parameter indicates the average difference between the observed and predicted values in the error distribution.
4. **Standard Deviation:** The standard deviation measures the dispersion or spread of the error values around the mean.
5. **Skewness**: Skewness measures the asymmetry of the error distribution. A positive skewness indicates a longer tail on the right side, while a negative skewness indicates a longer tail on the left side.
6. **Estimated Focal Length:** The estimated focal length is provided in both pixels and millimeters. It represents the distance between the camera lens and the image sensor.
7. **Control Error**: Control error refers to the discrepancy between the measured and true values of control points used in the photogrammetric process.

These parameters are compared across different flight altitudes and overlaps to analyze their variations and understand the impact of these factors on the accuracy and quality of the results.

As the flight altitude increases, the number of images required decreases. This is likely because a higher altitude provides a wider field of view, allowing for the capture of a larger area in a single image. Therefore, fewer images are needed to cover the same ground area.

At flight altitudes of 90 and 60 meters, increasing the forward and side overlap coverage and the number of images leads to an increase in the residual error. This means that the accuracy of the reconstructed model decreases as more problematic images are included in the dataset. These problematic images can negatively impact the geometry of the model, making it difficult to accurately identify points during the matching operation. As a result, the identification of internal and external matrices becomes less precise.

focal length. This could be due to the inclusion of images with varying focal lengths or distortion, which affects the estimation process. Furthermore, the control and check error rate for measured Ground Control Points (GCPs) also increases. This suggests that the accuracy of the GCPs used for georeferencing and ground truthing is compromised. The inclusion of problematic images may introduce errors in the identification and measurement of GCPs, leading to higher control and check error rates.

However, at a flight altitude of 120 meters, the behavior of the residual errors is slightly different. The minimum residual error is recorded for a forward and side overlap coverage of 70%.

This indicates that an optimum value is achieved at this overlap coverage, resulting in a more accurate reconstruction compared to other overlap percentages. Overall, these findings highlight the importance of carefully selecting flight altitudes, overlap coverage, and the number of images to ensure accurate and reliable results in photogrammetric projects. The focal distance estimated in this research serves as an indicator of how well the

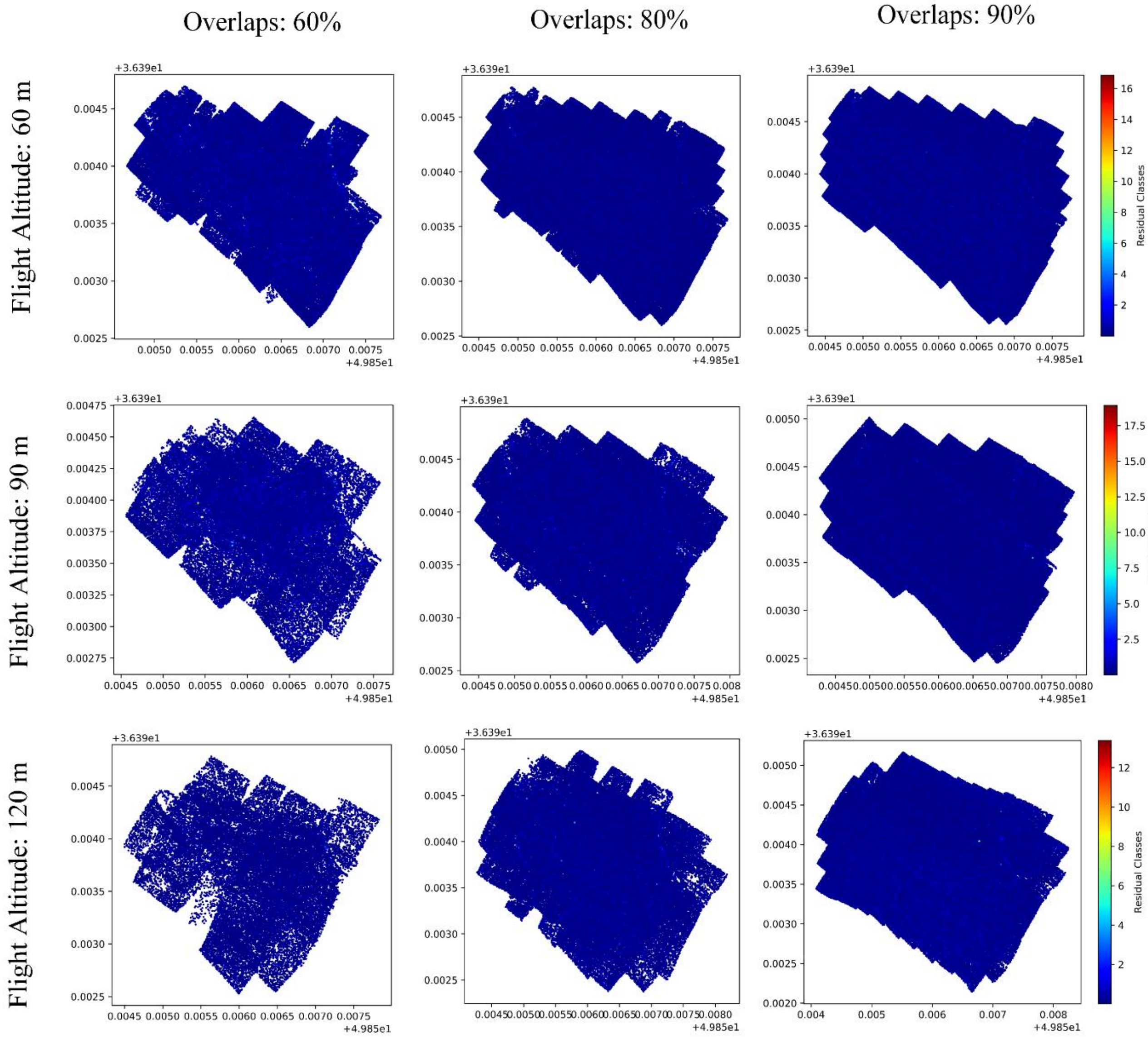

Figure 5. The residual error map for 3d sparse points cloud for flight altitudes of 60 m, 90 m, 120m and 60%, 70%, 80% forward and side overlaps

Additionally, the increase in the number of images and overlap coverage at these altitudes results in a decrease in the estimated calibration values were determined during the bundle adjustment process. Our findings reveal a reverse correlation between the residual errors and the estimated focal length. As

https://doi.org/10.5194/isprs-archives-XLVIII-4-W22-2025-59-2026

the residual errors of the sparse point cloud increase, the estimated focal length deviates further from the nominal values. In this study, the nominal focal length was set at 8.8 mm for each image capture. However, due to the presence of higher residual errors, the estimated focal length differs from this nominal value.

This suggests that the accuracy of the calibration process is influenced by the quality of the sparse point cloud. Higher residual errors indicate a less accurate reconstruction, which in turn affects the estimation of the focal length. The deviation from the nominal value indicates that the calibration values may not be as precise as desired. These findings emphasize the importance of minimizing residual errors in order to achieve more accurate calibration results and ensure the reliability of the estimated focal length.

To validate our claim, we focused on the sparse model and aimed to minimize the check error for Ground Control Points (GCPs). During our investigation, we found that the optimal values, with the minimum residual errors, were obtained at a flight altitude of 90 meters and a 60% overlap. At these specific flight conditions, we achieved a GCP control error of 0.0017 meters and a GCP check error of 0.00185 meters. These results provide further support for our assertion regarding the relationship between residual errors and the estimated focal length.

The fact that the minimum residual errors coincide with the optimal values for GCP control and check errors reinforces the idea that reducing residual errors leads to more accurate calibration and estimation of the focal length. This alignment between the findings further strengthens our claim and highlights the importance of minimizing residual errors in order to achieve reliable and precise results in photogrammetric projects.In summary, this section explores the relationship between flight altitude, overlap coverage, residual errors, and the estimated focal length in aerial UAV imaging. The findings indicate that specific flight altitudes and overlap coverage can

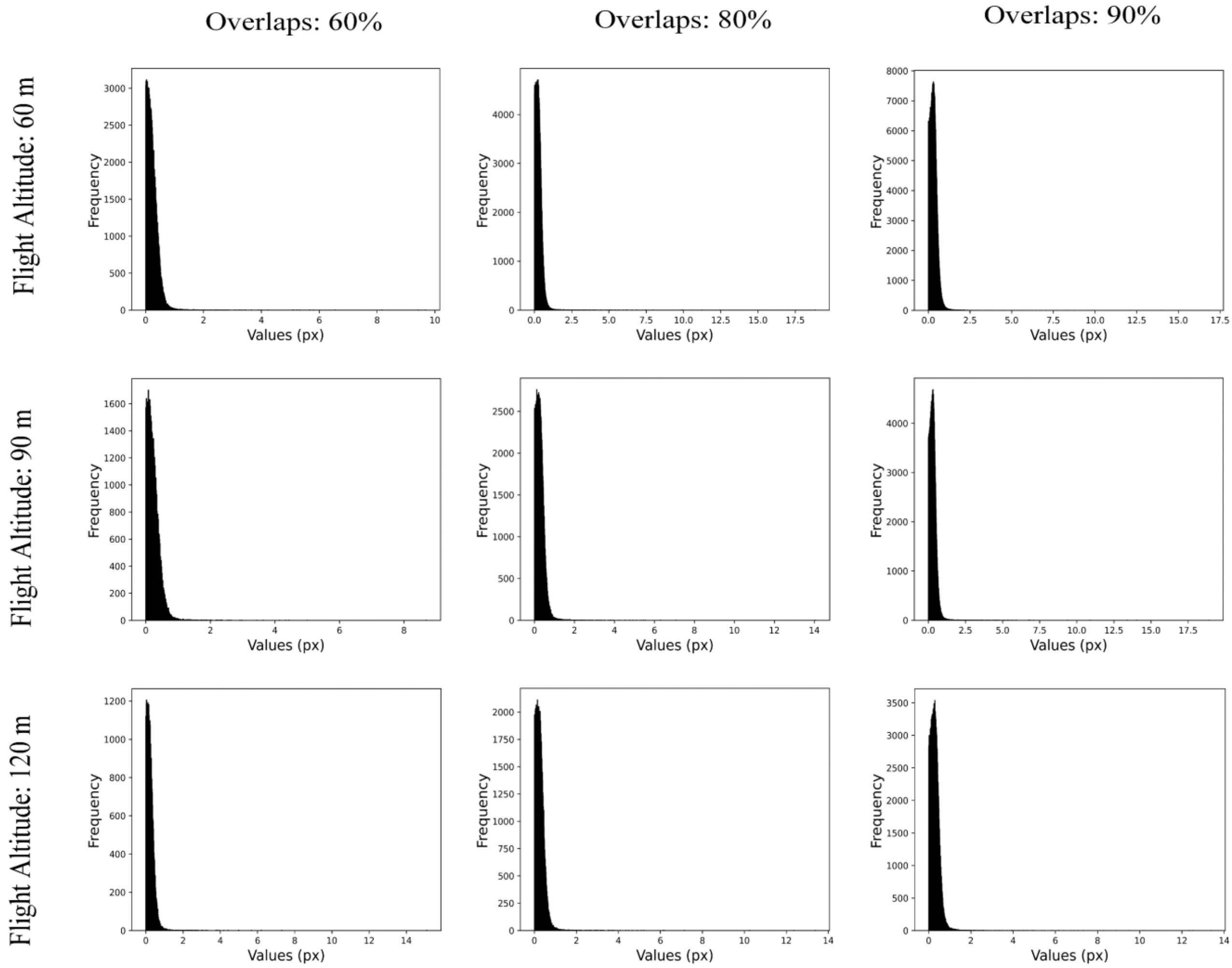

Figure 6. Distribution of residual errors for flight altitudes of 60 m, 90 m, 120m and 60%, 70%, 80% forward and side overlaps.

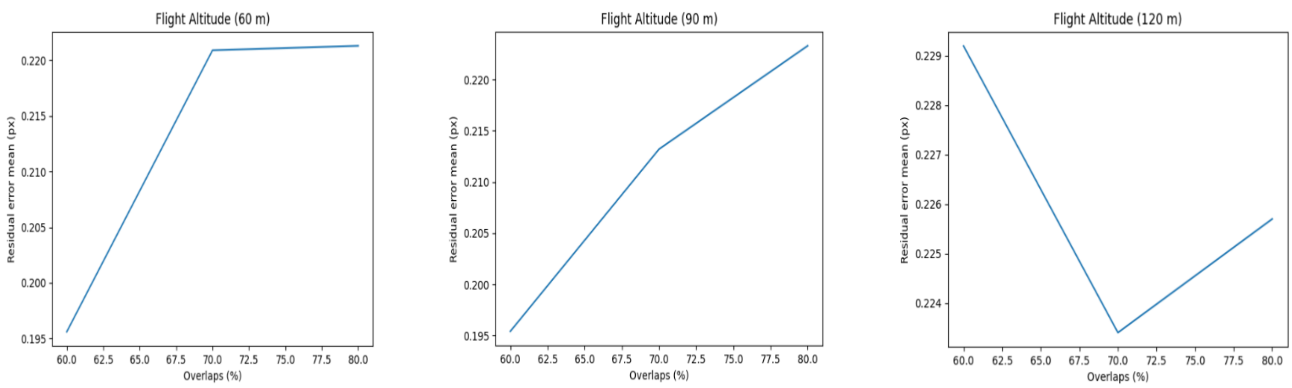

Figure 7. The plots of average of residual error for flight altitudes of 60 m, 90 m, 120m and 60%, 70%, 80% forward and side overlaps.

have a significant impact on the accuracy and quality of the results, particularly in terms of geometry and calibration.

5. Conclusion

Accurate 3D models derived from the combined utilization of photogrammetry and UAVs have gained significant importance across various industries. These models provide a wealth of valuable information and serve as powerful tools for a wide range of applications. UAV photogrammetry technology offers a cost-effective and efficient solution for generating these accurate 3D models. Among the key factors influencing the production of 3D models, flight altitude and forward and side over-laps play crucial roles. These factors directly impact the calibration parameters, thus influencing the overall accuracy and quality of the resulting 3D model.

In this study, we conducted experiments using a DJI phantom 4 pro UAV at flight altitudes of 60 m, 90 m, and 120 m, along with forward and side overlaps of 60%, 70%, and 80%. By modeling the residual errors of the 3D sparse points generated from tie points, we ar-rived at a noteworthy finding. The combination of a flight altitude of 90 m and a forward and side overlap of 60% yielded the best results in terms of residuals, with a value of 0.1954 pixels, as well as an estimated focal length of 8.7999 mm. These findings indicate that this particular combination optimizes the accuracy and precision of the 3D model.

The study reveals that increasing the flight altitude can result in a wider field of view and a decrease in the number of images required. However, it also leads to an increase in the Ground Sampling Distance (GSD), indicating a lower spatial resolution. Furthermore, the investigation highlights the influence of overlap coverage on the residual errors. It is observed that certain combi-nations of flight altitudes and overlaps can lead to high-er or lower residual errors. Optimal values for overlap coverage are identified, which result in the minimum residual errors. Additionally, the estimated focal length is found to be affected by the residual errors. As the residual errors increase, the estimated focal length devi-ates further from the nominal values, indicating potential calibration inaccuracies. Overall, these findings emphasize the importance of carefully selecting flight altitudes and overlap coverage to achieve more accurate results in terms of geometry and calibration in aerial UAV imaging projects.

In future research, we plan to further investigate this claim by exploring the effects of different flight alti-tudes and overlaps on calibration parameters. To achieve this, we intend to employ artificial neural net-works as a modeling tool. By leveraging the power of neural networks, we aim to optimize and determine the best calibration parameters for generating accurate 3D models. This approach will provide a more comprehensive understanding of the relationship between flight altitudes, overlaps, and calibration parameters, ultimately enhancing the quality and efficiency of UAV-based photogrammetry.

References

Agisoft LLC, 2019: Agisoft Metashape User Manual: Professional Edition. Version 1.6, 138 p.

Ahmed, S., El-Shazly, A., Abed, F., Ahmed, W., 2022: The influence of flight direction and camera orientation on the quality products of UAV-based SfM-photogrammetry. *Applied Sciences*, 12(20), 10492.

Albarelli, A., Rodolà, E., Torsello, A., 2010: Robust camera calibration using inaccurate targets. *Proc. British Machine Vision Conf.*, BMVA Press, 16.1-16.11.

Azmi, S.M., Ahmad, B., Ahmad, A., 2014: Accuracy assessment of topographic mapping using UAV image integrated with satellite images. *IOP Conf. Series: Earth and Environmental Science*, 18(1), 012015.

Barba, S., Barbarella, M., Di Benedetto, A., Fiani, M., Gujski, L., Limongiello, M., 2019: Accuracy assessment of 3D photogrammetric models from an unmanned aerial vehicle. *Drones*, 3(4), 79.

Curcio, A.C., Peralta, G., Aranda, M., Barbero, L., 2022: Evaluating the performance of high spatial resolution UAV-photogrammetry and UAV-Lidar for salt marshes: The Cádiz Bay study case. *Remote Sensing*, 14(15), 3582.

Cvišić, I., Marković, I., Petrović, I., 2022: Enhanced calibration of camera setups for high-performance visual odometry. *Robotics and Autonomous Systems*, 155, 104189.

Dai, F., Feng, Y., Hough, R., 2014: Photogrammetric error sources and impacts on modeling and surveying in construction engineering applications. *Visualization in Engineering*, 2, 1-14.

Elhadary, A., Rabah, M., Ghanim, E., Mohie, R., Taha, A., 2022a: The influence of flight height and overlap on UAV imagery over featureless surfaces. *MEJ-Mansoura Engineering Journal*, 47(2), 34-42.

Elhadary, A., Rabah, M., Ghanim, E., Mohie, R., Taha, A., 2022b: The Influence of Flight Height and Overlap on UAV Imagery Over Featureless Surfaces. *NRIAG Journal of Astronomy and Geophysics*, 11(1), 210-223.

Galkin, B., Kibilda, J., DaSilva, L.A., 2017: Coverage analysis for low-altitude UAV networks in urban environments. *GLOBECOM 2017-2017 IEEE Global Communications Conf.*, IEEE, 1-6.

Goncalves, J.A., Henriques, R., 2015: UAV photogrammetry for topographic monitoring of coastal areas. *ISPRS Journal of Photogrammetry and Remote Sensing*, 104, 101-111.

Hanning, T., Graf, S., Kellner, M., 2005: Re-projective vs. projective camera calibration: effects on 3D-reconstruction. *IEEE International Conf. on Image Processing 2005*, 2, II-1170.

Hong, C., Daiqiang, W., Yuqing, C., 2021: Research on the Influence of Calibration Image on Reprojection Error. *2021 International Conf. on Big Data Engineering and Education (BDEE)*, 60-66.

Imangholiloo, M., Saarinen, N., Markelin, L., Rosnell, T., Näsi, R., Hakala, T., et al., 2019: Characterizing seedling stands using leaf-off and leaf-on photogrammetric point clouds and hyperspectral imagery acquired from unmanned aerial vehicle. *Forests*, 10(5), 415.

Karami, A., Menna, F., Remondino, F., 2022: Combining photogrammetry and photometric stereo to achieve precise and complete 3D reconstruction. *Sensors*, 22(21), 8172.

Ma, S., Zhang, K., 2022: Low-altitude photogrammetry and remote sensing in UAV for improving mapping accuracy. *Mobile Information Systems*, 2022, 1-8.

Moyano, J., Nieto-Julián, J.E., Bienvenido-Huertas, D., Marín-García, D., 2020: Validation of close-range photogrammetry for architectural and archaeological heritage: Analysis of point density and 3D mesh geometry. *Remote Sensing*, 12(21), 3571.

Rokhmana, C.A., Tjahjadi, M.E., Agustina, F.D., 2019: Cadastral surveys with non-metric camera using UAV: a feasibility study. *KnE Engineering*, 227-237.

Rueda-Ayala, V.P., Peña, J.M., Höglind, M., Bengochea-Guevara, J.M., Andújar, D., 2019: Comparing UAV-based technologies and RGB-D reconstruction methods for plantheight and biomass monitoring on grass ley. *Sensors*, 19(3), 535.

Ruzgienė, B., Berteška, T., Gečyte, S., Jakubauskienė, E., Aksamitauskas, V.Č., 2015: The surface modelling based on UAV Photogrammetry and qualitative estimation. *Measurement*, 73, 619-627.

Shahbazi, M., Sohn, G., Théau, J., Menard, P., 2015: Development and evaluation of a UAV-photogrammetry systemfor precise 3D environmental modeling. *Sensors*, 15(11), 27493-27524.

Wang, F., Zou, Y., Castillo, E.D.R., Lim, J.B.P., 2022: Optimal UAV Image Overlap for Photogrammetric 3D Reconstruction of Bridges. *IOP Conf. Series: Earth and Environmental Science*, 1101(2), 022052.

Wierzbicki, D., Nienaltowski, M., 2019: Accuracy analysis of a 3D model of excavation, created from images acquired with an action camera from low altitudes. *ISPRS International Journal of Geo-Information*, 8(2), 83.

Zahran, S., Moussa, A., El-Sheimy, N., 2019: Enhanced drone navigation in GNSS denied environment using VDM and hall effect sensor. *ISPRS International Journal of Geo-Information*, 8(4), 169.

This contribution has been peer-reviewed.
https://doi.org/10.5194/isprs-archives-XLVIII-4-W22-2025-59-2026 | © Author(s) 2026. CC BY 4.0 License.